Pattern Recognition 42 (2009) 3324 – 3337

Contents lists available at ScienceDirect

Pattern Recognition

journal homepage: www.elsevier.com/locate/pr

Development of a Sigma–Lognormal representation for on-line signatures

Christian O'Reilly*, Réjean Plamondon

Laboratoire Scribens, Département de Génie Électrique, École Polytechnique de Montréal, C.P. 6079, Succursale Centre-Ville, Montréal, QC, Canada H3C 3A7

ARTICLE INFO

Article history:
Received 22 August 2008
Accepted 15 October 2008

Keywords:
Signature representation
Sigma–Lognormal
Parameter extraction
Handwriting processing

ABSTRACT

This paper proposes an on-line signature representation based on Sigma–Lognormal modeling. It briefly overviews the prior art published on signature modeling and on human movement analysis for handwriting. Then it presents the Sigma–Lognormal paradigm and gives the key steps for the development of a completely automatic parameter extractor for complex human movements. Results of its application on signatures from a proprietary database and from the SVC2004 database are reported and analyzed in regards of the curve fitting quality. Other possible applications and future works are also suggested.

1. Introduction

As one of many research areas included in the field of pattern recognition, handwriting recognition shares with its mother discipline a same general framework. That is, its analysis can be divided in three general topics. In the context of the development of a system, these can be formulated as questions to be addressed: (1) How individual patterns (i.e., each specimen of letters, words, or signatures) will be represented? (2) How classes (i.e., abstraction of letters, words, or signatures) will be described? (3) And finally, by which means patterns will be associated to classes? This paper is addressing the first of these questions in the specific context of signatures verification.

The next section presents a short overview of the previous works published on signature representation. Theories and frameworks developed for the analysis of human movement are also discussed since a signature representation based on a physiological model is proposed. The most important aspects of the chosen model are then summed up. Section 3 addresses the important question of extracting parameters from experimental data. It is followed by a presentation of the results obtained on human signatures. Finally, Section 5 gives propositions for other possible applications and for future works.

2. Previous works

2.1. Signature representation

Signature representation depends heavily on the type of device used for data acquisition. Generally, static (off-line) signature verification systems use imaging devices such as scanners and cameras providing gray scaled images. Although, off-line systems have definitive advantages for some applications (e.g., forensic analysis, check verification), they are more challenging to design than dynamic (on-line) signature verification systems [1] because of the relative scarcity of information they have to deal with. Therefore, dynamic signature verification is more often considered as a biometric measure for resources access control. This paper deals with the latter type of system and focuses specifically on dynamic signature representation.

On-line systems most often use graphic digitizers, tablet PCs or PDAs as acquisition devices. These produce time varying data about pen tip kinematics, pressure, and orientation. After proper preprocessing (e.g., filtering, normalization, re-sampling, truncation), these input signals can be used directly, be fitted by mathematical time-varying functions, or be modified (e.g., differentiated, integrated, combined, transformed) to calculate more informative signals. This approach is said to be function-based (e.g., Refs. [2,3]) and is often associated with different sorts of temporal axis deformation techniques [3–19] to model signature variability.

A second approach is based on the constitution of a feature vector to encode signature's characteristics [1,20,24,25]. Feature extraction from acquired signals is performed using various techniques such as hidden Markov models [2,26–37] and Markov chains [38], spectrum analysis [39,40], wavelet decomposition [41,42], and cross or regular correlation [4,8,13]. More basic global features are also used such as total signing time, signature dimensions and dimension ratios, amount of zero crossings of different signals, maximal, minimal, average, and dispersion of velocity, acceleration, curvature, pressure, or pen orientation. Dimensionality of feature vectors is generally moderately large—about 50—and can be reduced by defining a user specific feature subset [21,23,43]. This selection process or a vector component weighing [22] has also been used to model specific user's stabilities.

* Corresponding author.
E-mail addresses: christian.oreilly@polymtl.ca (C. O'Reilly), rejean.plamondon@polymtl.ca (R. Plamondon).

0031-3203/$ - see front matter © 2008 Elsevier Ltd. All rights reserved.
doi:10.1016/j.patcog.2008.10.017

Features are often separated in different classes regarding that they are shape or dynamics-related [40,44], skilled or random forgery discriminative [45], locally or globally descriptive, or of a continuous, discrete or quantized nature. In most case, systems designer try to incorporate different type of complementary features by concatenating them in a vector or through some kind of fusions [16].

Global features can be made local if applied to elements of a segmented signature. Using local features to perform a stoke-by-stroke signature comparison is sometime seen as a different approach which is then referred as a stoke-based approach (e.g., Refs. [11,46]). Although, this decomposition in more basic elements (e.g., strokes, components, segments, strings) raises a segmentation problem [12,17,45,47–49], it has shown to lay good results.

Finally, it is worth mentioning that these distinct approaches may either be used by themselves or be combined [21,44,47] to best capture signatures writer's specificities from input data.

2.2. Human movement modeling

In this work, an approach using a physiological model of human movement production for the generation of signatures has been adopted as a representation scheme. This choice is motivated by the hypothesis that it would lead to an improved characterization of the signee's hidden specificities. It also has the advantage of being invariant in regard of cultural or language differences, whereas systems based on visual characteristics often need to be tailored for Chinese, Arabic, European, or American signatures. The next paragraphs overview the previously proposed models and lay down some ground rules that has been used to choose an adequate model signature representation.

Several computational models have been proposed to tentatively explain how the central nervous system generates and controls the kinematics of human movements. Some of them describe a movement with analytical expressions [50–53], while others proceed through the numerical resolution of a system of differential equations [54–60]. The utilization of an equilibrium hypothesis [61,62] has also been firmly rooted from a neurophysiologic point of view. Finally, the usage of a minimum principle [63] as a basis for solving indeterminacy in human movement control has also been widely discussed in the literature. It has been tested using different variables to minimize (e.g., movement time [64], acceleration [65], jerk [66], snap [67], torque changes [68]) and has also been applied specifically to handwriting in some cases [67,75].

Following Hollerbach's pioneer work [69], Gangadhar et al. have also proposed [70] an oscillatory neuromotor model for the analysis and synthesis of handwriting along with a nice survey of some competing model (see Ref. [71] for Schomaker's model, Ref. [72] for Kalveram's model, Refs. [53,73] for Delta–Lognormal model, and Ref. [74] for the AVITEWRITE model).

Facing such variety of choices for a model of representation, some guidelines have to be devised when it comes to incorporate one into the design of a signature verification system. First, the type of signal used for representation should be chosen. Wolpert et al. [76] point out that kinematics signals should be preferred over kinetics ones. Moreover, the study published in Ref. [77] indicates that the velocity signals have the most discriminative kinematic space for signature verification. Thus, velocity oriented models has been preferred. Furthermore, four additional criterions have been considered: (1) the model should have an analytical form for an easy use in analysis as well as in synthesis; (2) it also must be implementable in a parameter extraction algorithm; (3) it should make the analysis of kinematics as straightforward as possible, given that data are obtained through a digitizer; (4) finally, it should be able to represent complex movements. In this overall context, the Sigma–Lognormal model seemed a good candidate.

2.3. The Sigma–Lognormal model

The kinematics theory of rapid human movements from which the Delta–Lognormal ($\Lambda\Lambda$) and the Sigma–Lognormal ($\Sigma\Lambda$) models were developed has been first introduced in Ref. [53], [73]. For briefness reasons, only the basis of $\Sigma\Lambda$ model will be overviewed here.

The Sigma–Lognormal model considers the resulting speed of a neuromuscular system action as having a lognormal shape scaled by a command parameter (D) and time-shifted by the time occurrence of the command (t_0) (see Eq. (1)). Moreover, because it represents the movement as happening along a pivot, the angular position can be calculated as shown in Eq. (2) where the set of parameters P_j is defined in Eq. (3). Finally, $erf(x)$ is the error function, as defined by Eq. (4)[1]:

$$|\vec{v}_j(t;P_j)| = D_j \Lambda(t-t_{0j};\mu_j,\sigma_j^2) = \frac{D_j}{\sigma(t-t_{0j})\sqrt{2\pi}} \exp\left(\frac{[\ln(t-t_{0j})-\mu_j]^2}{-2\sigma_j^2}\right) \tag{1}$$

$$\phi_j(t;P_j) = \theta_{sj} + \frac{\theta_{ej}-\theta_{sj}}{D_j}\int_0^t |\vec{v}_j(\tau;P_j)|\,\mathrm{d}\tau = \theta_{sj} + \frac{\theta_{ej}-\theta_{sj}}{2}\left[1+erf\left(\frac{\ln(t-t_{0j})-\mu_j}{\sigma_j\sqrt{2}}\right)\right] \tag{2}$$

$$P_j = [D_j \;\; t_{0j} \;\; \mu_j \;\; \sigma_j \;\; \theta_{sj} \;\; \theta_{ej}]^t \tag{3}$$

$$erf(x) = \frac{2}{\sqrt{\pi}}\int_0^x \mathrm{e}^{-t^2}\,\mathrm{d}t \tag{4}$$

The synergy emerging from the interaction and coupling of many of these neuromuscular systems results in the sequential generation of complex movements. As shown by Eq. (5), this is modeled using a vectorial summation of lognormals:

$$\vec{v}(t) = \vec{\Sigma}\Lambda(t;P) = \sum_{j=1}^{M}\vec{v}_j(t;P_j) \tag{5}$$

$$P = [P_1^t \;\; P_2^t \;\; \ldots \;\; P_j^t \;\; P_M^t]^t \tag{6}$$

The velocity in the Cartesian space can be calculated, as shown in Eqs. (7) and (8), and then used to obtain positions versus time as done in Eqs. (9) and (10):

$$v_x(t;P) = \sum_{j=1}^{M}|\vec{v}_j(t;P_j)|\cos(\phi_j(t;P_j)) \tag{7}$$

$$v_y(t;P) = \sum_{j=1}^{M}|\vec{v}_j(t;P_j)|\sin(\phi_j(t;P_j)) \tag{8}$$

$$x(t;P) = \int_0^t v_x(\tau;P)\,\mathrm{d}\tau \tag{9}$$

$$y(t;P) = \int_0^t v_y(\tau;P)\,\mathrm{d}\tau \tag{10}$$

Alternatively, for better performances, $x(t)$ and $y(t)$ signals can be computed directly from lognormal parameters with Eqs. (11) and (12) which are demonstrated in Appendix B.

$$x(t;P) = \sum_{j=1}^{M}\frac{D_j}{\theta_{ej}-\theta_{sj}}\{\sin(\phi_j(t;P_j)) - \sin(\theta_{sj})\} \tag{11}$$

[1] Please note that, for reference purpose, the mathematical notation used throughout the text is described in Appendix A.

$$y(t;P)=\sum_{j=1}^{M}\frac{D_j}{\theta_{ej}-\theta_{sj}}\{-\cos(\phi_j(t;P_j))+\cos(\theta_{sj})\} \tag{12}$$

These signals can also be conveniently represented as a single complex signal as shown in Eq. (13). The polar complex expression may be useful to compute both Cartesian coordinates efficiently. However, Eqs. (11) and (12) seem to be computed faster in Matlab.

$$\begin{aligned} s(t;P) &= x(t;P)+\mathrm{i}y(t;P)\\ &= \sum_{j=1}^{M}\frac{D_j}{\theta_{ej}-\theta_{sj}}[\{\sin(\phi_j(t;P_j))\\ &\quad -\sin(\theta_{sj})\}-j\{\cos(\phi_j(t;P_j))+\cos(\theta_{sj})\}]\\ &= \sum_{j=1}^{M}\frac{\mathrm{i}D_j}{\theta_{ej}-\theta_{sj}}\{\mathrm{e}^{-\mathrm{i}\theta_{sj}}-\mathrm{e}^{-\mathrm{i}\phi_j(t;P_j)}\} \end{aligned} \tag{13}$$

3. ΣΛ Parameter extraction

3.1. Extraction generalities

Parameter extraction is an essential step for $\Sigma\Lambda$ signature representation. Many attempts have been conducted to develop algorithms for that purpose. Excellent results have been achieved on simple rapid strokes [78] and some preliminary results have been reported on complex movements [79]. However, no algorithm has been shown to be robust and flexible enough to process automatically large databases of complex human movements like handwritten signatures. To partly address this problem, we present a powerful $\Sigma\Lambda$ parameter extractor, based on the XZERO algorithm [78]. Its general structure is shown in Fig. 1.

The proposed extractor proceeds in two different modes. It starts in the first one, where lognormal equations are estimated and optimized in the order of their time occurrence. This mode is preferred because it is believed to provide a better framework to isolate each lognormal. It is designed so that, while estimating the Jth stroke,[2] it minimizes the superposition effects from direct neighboring lognormals (i.e., stroke $J-1$ and $J+1$) by removing their extracted value. However, if the end of the signals is reached without having obtained a satisfactory signal to noise reconstruction ratio (SNR), the extractor toggles in the second mode where it process lognormal strokes in descending order of their area under the curve that is of the importance of their effect on the movement.

The Algorithm 1 shows the sequence of operations executed in both modes. In this code, ExtractFirstMode(…) and ExtractMaxImportantMode(…) perform operations included in all four modules following the *signal update* in Fig. 1. The first function locates strokes in order of their timing occurrence while the latter does it in order of their importance in terms of their area under the curve. SubtractStroke(X,Y,$P(j)$) and AddStroke(X,Y,$P(j)$), respectively, performs a vectorial subtraction and addition of the Jth lognormal stroke to the (X,Y) signals. Finally, CalculateSNR(X,Y,P,J) computes the SNR between (X,Y) and the signal synthesized from parameter matrix P. This SNR is computed[3] on the interval defined by the time occurrence of the two velocity inflection points of the Jth lognormal.[4]

Algorithm 1. General algorithm for extraction.

```
// FIRST MODE OF EXTRACTION
SNRmin          = 30                    // Threshold to reach (in dB) before passing to the next stroke.
IterMax         = 3                     // Maximal nb. of iterations before passing to the next stroke.
I               = 0                     // Number of iteration performed while estimating mode ID.
J               = 1                     // Mode ID of the currently under estimation stroke.
Xn, Yn                                  // Numerical signal to be estimated.
Xs              = Xn                    // X stroke of the input signal of the extraction process
Ys              = Yn                    // Y stroke of the input signal of the extraction process
P                                       // Lognormal parameter matrix
P(J) = ExtractFirstMode(Xs, Ys)         // Estimating first mode . . .
WHILE CriterionMode1
  [Xs Ys]       = SubtractStroke(Xs, Ys, P(J))
  P(J+1)        = ExtractFirstMode(Xs, Ys);   // Estimating J+1th mode without
                                              // the effect of the 1 to Jth modes
  [Xs Ys]       = AddStroke(Xs, Ys, P(J))
  [Xs Ys]       = SubtractStroke(Xs, Ys, P(J+1))
  P(J)          = ExtractFirstMode (Xs, Ys)   // Estimating Jth mode without the
                                              // effect of 1 to J-1th and J+1th mode
  SNR           = CalculateSNR(Xn, Yn, P, J)
  IF (SNR > SNRmin) OR (I > IterMax)
      [Xs Ys] = AddStroke(Xs, Ys, P(J+1))
      [Xs Ys] = SubtractStroke(Xs, Ys, P(J))
      J = J+1
      I = 0
      P(J) = ExtractFirstMode (Xs, Ys)  // Estimating J+1th mode without the
                                        // effect of 1 to J-1th modes
  ELSE
```

[2] In the context of the Delta-Lognormal model, strokes are defined as the result of two synergetic and antagonist lognormal equations. However, in this paper, and in the context of the Sigma-Lognormal model in general, a stroke is considered as being a movement resulting from a single lognormal equation.

[3] More details on the SNR computation can be found in Section 4.1.1.

[4] An alternative graphical explanation of the extraction process of the first mode can be found in Section 3.7 of Ref. [80].

```
    I = I+1
  END
END


// SECOND MODE OF EXTRACTION
J               = J +1
SNR             = CalculerSNRvxy(T_n, T_a);
MaxSNR          = SNRCalculer;                          // Maximal SNR obtained so far
NoModeMaxSNR    = size(T_a.param, 1);                   // ID of mode under extraction when MaxSNR
                                                        // was obtained
WHILE CriterionMode2
  P(J)          = ExtractMaxImportantMode(Xs, Ys)
  [Xs Ys]       = SubtractStroke(Xs, Ys, P(J))
  LastSNR       = SNR
  SNR           = CalculateSNR(Xn, Yn, P, J)
  IF SNR > MaxSNR                                       // Keeping track of when the best SNR was obtained
      MaxSNR = SNR
      NoModeSNRMax = J
  ELSE IF SNR < (MaxSNR-5)                              // Performance are degrading, exit extraction.
      P = P(1:NoModeMax)
      RETURN
  END


  J = J+1
END
```

3.2. Stroke identification

To estimate the $\Sigma\Lambda$ parameters, lognormal strokes must first be localized in the velocity magnitude profile, resulting in a sequence of the five characteristic points. Their definition is given in Table 1.

Because noise can generate false characteristic point series, some kind of pruning is needed to retain only series that are thought to be meaningful. Two criterions are applied independently of the extraction mode. The first one, specify that the area under the curve delimited by p_1 and p_5 must be greater than the mean minus one standard deviation of the area under the curve of all computed series. This threshold determination technique has the advantage of being automatically adjusted for every specimen of signature. This is an improvement over using an absolute threshold such as the minimal value of D proposed in Ref. [80]. The second criterion ensures that the maximum value of a series (i.e., v_{t3}) is not more than λ times smaller than the maximal value of v_t. A $\lambda = 15$ has been taken for the results presented in this paper. Finally, a third condition is applied only in the first mode. It states that the value of t_3 of a series taken to estimate a new lognormal should be greater than those used previously. This assures a continuous progression of the algorithm.

3.3. XZERO estimation

The algorithm we propose for complex movement parameter extraction is based on a generalization of the XZERO algorithm. Therefore, XZERO will first be introduced. For the interested reader, Ref. [78] is a more comprehensive presentation of this topic.

XZERO has been designed to improve the estimation of the $\Lambda\Lambda$ parameters of rapid human movements. This kind of movements is a simplified variation of $\Sigma\Lambda$ patterns. In this case, agonist and antagonist neuromuscular systems are considered as being exactly opposed.

$$|\vec{v}(t)| = |\vec{v}_1(t)| - |\vec{v}_2(t)| = D_1\Lambda(t-t_0;\mu_1,\sigma_1^2) - D_2\Lambda(t-t_0;\mu_2,\sigma_2^2) \quad (14)$$

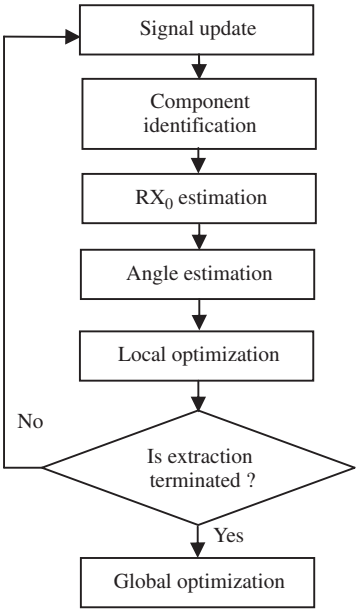

Fig. 1. Basic structure of the extractor.

XZERO exploits the properties of zero crossing points of the first and the second derivatives of a single time-shifted and weighted lognormal equation. Their analytical expression is given by Eqs. (15) and (16), where k is defined as in Eq. (17):

$$\dot{\Lambda}(t-t_0) = -\frac{\Lambda(t-t_0)}{\sigma(t-t_0)}(\sigma+k) \quad (15)$$

$$\ddot{\Lambda}(t-t_0) = -\frac{\Lambda(t-t_0)}{\sigma^2(t-t_0)^2}(k^2+3k\sigma+2\sigma^2-1) \quad (16)$$

$$k = \frac{\ln(t-t_0)-\mu}{\sigma} \quad (17)$$

Table 1
Definition of the five characteristic points

i	Definition (p_i)	Numerical value (p_{i_n})
1	Lognormal stroke beginning	First point preceding p_{3_n} which is a local minimum or has a magnitude of less than 1% of v_{3_n}
2	First inflexion point	First $\dot{v}_{t\_n}$ zero crossing before p_{3_n}
3	Local maximum of the lognormal stroke	Local maximum of v_{t_n}
4	Second inflexion point	First $\dot{v}_{t\_n}$ zero crossing after p_{3_n}
5	Lognormal stroke ending	First point following p_{3_n} which is a local minimum or has a magnitude of less than 1% of v_{3_n}

Non-trivial zeros of Eqs. (15) and (16) can be used to obtain the time occurrence and the magnitude of the points p_2, p_3, and p_4. Furthermore p_1 and p_5 can be chosen so that they define an interval containing 99.97% of the surface under the lognormal curve. The corresponding analytical expressions are given by Eqs. (18) and (19) with the a_i parameter given by Eq. (20):

$$t_i = t_0 + e^{\mu} e^{-a_i}, \quad i \in \{1, 2, \ldots, 5\} \tag{18}$$

$$v_{ti} = \frac{D}{\sqrt{2\pi}} e^{-\mu} \sigma^{-1} e^{(a_i - (a_i^2/2\sigma^2))}, \quad i \in \{1, 2, \ldots, 5\} \tag{19}$$

$$a_1 = 3\sigma \tag{20a}$$

$$a_2 = 1.5\sigma^2 + \sigma\sqrt{0.25\sigma^2 + 1} \tag{20b}$$

$$a_3 = \sigma^2 \tag{20c}$$

$$a_4 = 1.5\sigma^2 - \sigma\sqrt{0.25\sigma^2 + 1} \tag{20d}$$

$$a_5 = -3\sigma \tag{20e}$$

Using theses relations, it can be shown that σ can be estimated solving the non-linear expression (21):

$$\frac{t_{3\_n} - t_{1\_n}}{t_{5\_n} - t_{1\_n}} = \frac{e^{-a_3} - e^{-a_1}}{e^{-a_5} - e^{-a_1}} \tag{21}$$

Then, t_0, D and μ can be calculated as shown in Eqs. (22)–(24). These expressions are given in a generalized form. In the particular case of the XZERO algorithm, $i = 3$ in Eqs. (22) and (23) and $\{i = 4, j = 2\}$ in Eq. (24):

$$t_0 = t_{i\_n} - e^{\mu} e^{-a_i} \tag{22}$$

$$D = \sqrt{2\pi} v_{ti\_n} e^{\mu} \sigma e^{((a_i^2/2\sigma^2) - a_i)} \tag{23}$$

$$\mu = \ln\left\{\frac{t_{i\_n} - t_{j\_n}}{e^{-a_i} - e^{-a_j}}\right\} \tag{24}$$

Considering that the antagonist contribution is non-significant in regard of the agonist's one, Eqs. (21)–(24) are used directly on $|v(t)|$ to calculate the agonist parameters. This yields an approximation of $|v_1(t)|$. Subtracting it from $|v(t)|$ gives an estimation of $|v_2(t)|$. This signal is then used to extract antagonist parameters in a somewhat similar fashion then what has been done for the agonist lognormal.

XZERO has been shown to lay very good results at extracting $\Delta\Lambda$ parameters. However, it cannot be used as-is on complex movements. The Robust XZERO algorithm (RX_0) achieves this goal by generalizing the overall methodology [78].

3.4. Robust XZERO estimation

Eqs. (20a)–(20e) are at the basis of the RX_0 estimation. These relationships use only velocity amplitude signals. Thus, for every lognormal stroke, four speed related parameters (i.e., t_0, D, μ and σ) have to be estimated by the RX_0 algorithm. Angular parameters are dealt with afterward.

Table 2
Expression of σ depending on the available v_{ti} constraints

Available v_{ti_n}	σ value
v_{t2_n} and v_{t3_n}	$\sqrt{-2 - 2\ln(\beta_{23}) - \frac{1}{2\ln(\beta_{23})}}$
v_{t2_n} and v_{t4_n}	$\sqrt{2\sqrt{1 + \ln^2(\beta_{42})} - 2}$
v_{t3_n} and v_{t4_n}	$\sqrt{-2 - 2\ln(\beta_{43}) - \frac{1}{2\ln(\beta_{43})}}$
Only one v_{ti_n}	$\frac{t_{2\_n} - t_{3\_n}}{t_{4\_n} - t_{2\_n}} = \frac{e^{-a_4} - e^{-a_3}}{e^{-a_4} - e^{-a_2}}$

To reach that goal, six constraints are available from the p_2, p_3 and p_4 expressions. These are of the form $v_{ti\_a} = v_{ti\_n}$ or $t_{i\_a} = t_{i\_n}$ where the left-hand term has an analytical expression as given by Eqs. (18) and (19) and the right-hand term has a numerical value obtained from the velocity profile, as described in the third column of Table 1.

From these six constraints, 15 different four elements combinations are available to estimate the lognormal parameters. However, it can be shown that there is a redundant constraint in sets using all three v_{ti} values, so there are in fact only 12 sets that are useful.

D, t_0, and μ can be calculated as shown in Eqs. (22)–(24), taking whatever v_{ti_n} and t_{i_n} values in hand. As for σ, its expression depends on the available v_{ti} values as presented in Table 2 where the β_{ij} parameter used in this table is a ratio of v_{ti_n} on v_{tj_n}. Moreover, the three sets of constraints using only one v_{ti} need numerical resolution. To stick with closed-form solutions only, these combinations will be discarded, leaving nine useful sets that will be used to lay nine different lognormal parameter estimations. The estimation which minimizes the least-square reconstruction error of $|v(t)|$ is kept as the initial solution output from RX_0 algorithm.

3.5. Parameter variability restriction

To increase robustness, the a priori knowledge on the possible variability of the parameters has to be used in the estimation process to narrow the range of possible solutions to the parameter estimation problem. So far, variability restriction has only been applied to the σ and μ parameters. Let's consider the general case where the parameter variability is defined as in Eq. (25):

$$\mu \in [\mu_-, \mu_+] \tag{25a}$$

$$\sigma \in [\sigma_-, \sigma_+] \tag{25b}$$

The goal here is to use this knowledge to correct the p_{2_n}, p_{3_n}, and p_{4_n} values when noise or superposition drift these points out of the region they should be with respect to the variability of μ and

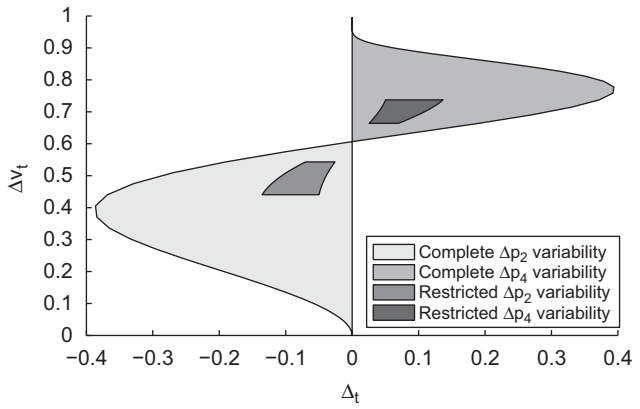

Fig. 2. Example of parameter variability limitation ($\mu \in [-2.0,-1.0]$ and $\sigma \in [0.2,0.5]$).

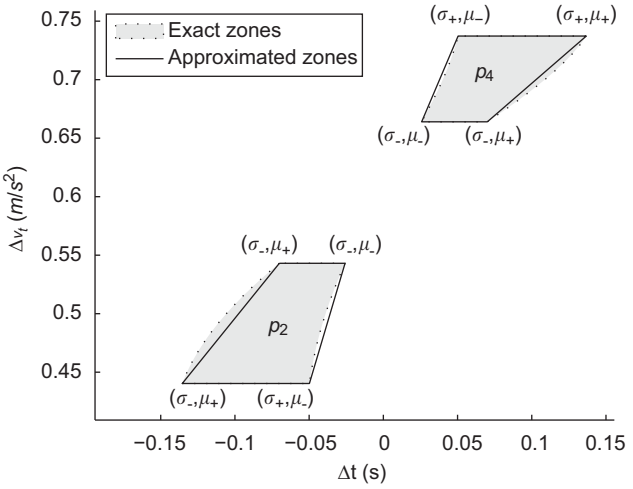

Fig. 3. Quadrilateral zone approximation.

σ. Because the value of p_{3_n} has been found to be the more reliable than the p_{2_n} and p_{4_n} positions, these latter are limited relatively to p_{3_n}.

Eqs. (26) and (27) define the relative position of a point from p_{3_n} and Eqs. (28) and (29) give the corresponding analytical expressions for p_2 and p_4.

$$\Delta t = t - t_3 \tag{26}$$

$$\Delta v_t = v_t / v_{t3} \tag{27}$$

$$\Delta t_2 = t_3 - t_2 = e^{\mu} e^{-\sigma^2}(1 - e^{-(\sigma/2)(\sigma+\sqrt{\sigma^2+4})}) \tag{28a}$$

$$\Delta t_4 = t_3 - t_4 = e^{\mu} e^{-\sigma^2}(1 - e^{-(\sigma/2)(\sigma-\sqrt{\sigma^2+4})}) \tag{28b}$$

$$\Delta v_{t2} = \frac{v_{t2}}{v_{t3}} = e^{(1/4)(\sigma^2-\sigma\sqrt{\sigma^2+4}+2)} \tag{29a}$$

$$\Delta v_{t4} = \frac{v_{t4}}{v_{t3}} = e^{(1/4)(\sigma^2-\sigma\sqrt{\sigma^2+4}+2)} \tag{29b}$$

The variability of σ and μ limits the possible localization of p_{2_n} and p_{4_n} as shown in Fig. 2. Furthermore, if the variability of σ is restricted in either of the intervals [0, 0.65] or [0.65, $+\infty$], these zones can be approximated by quadrilaterals as shown on Fig. 3.

Eqs. (30a)–(30d) give the conditions for a sample from v_{t_n} to be a valid candidate for p_{2_n}. The $f(\dots)$ function used in these expressions is defined in Eq. (32). Analogous equations can be developed for p_{4_n}. Using these relationships, noisy values of p_{2_n} and p_{4_n} can be corrected and a reliability confidence measurement can be obtained considering the importance of the correction made. Table 3 presents typical results of the utilization of the parameter variability restrictions on p_{2_n} and p_{4_n} accuracy:

Table 3
Average error (in %) on p_2 and p_4 before and after the utilization of the parameter variability restrictions

	$t_{\_n}$	v_{t_n}
Extracted p_2	5.1	46.2
Corrected p_2	2.5	11.0
Extracted p_4	4.6	19.8
Corrected p_4	2.2	5.4

$$\Delta v_{t\_n} \leqslant f(\Delta t\_n, \Delta p_2(\sigma_+,\mu_+), \Delta p_2(\sigma_-,\mu_+)) \tag{30a}$$

$$\Delta v_{t\_n} \leqslant f(\Delta t\_n, \Delta p_2(\sigma_-,\mu_+), \Delta p_2(\sigma_-,\mu_-)) \tag{30b}$$

$$\Delta v_{t\_n} \geqslant f(\Delta t\_n, \Delta p_2(\sigma_+,\mu_-), \Delta p_2(\sigma_-,\mu_-)) \tag{30c}$$

$$\Delta v_{t\_n} \geqslant f(\Delta t\_n, \Delta p_2(\sigma_+,\mu_+), \Delta p_2(\sigma_+,\mu_-)) \tag{30d}$$

$$\Delta p_2(\sigma,\mu) = (\Delta t_2(\sigma,\mu), \Delta v_{t2}(\sigma,\mu)) \tag{31}$$

$$f(x,(x_1,y_1),(x_2,y_2)) = \frac{y_2-y_1}{x_2-x_1}(x-x_1)+y_1 \tag{32}$$

3.6. Angle estimation

The parameters D, t_0, μ, and σ having been estimated, the angular parameters θ_s and θ_e remain to be evaluated. From the hypothesis that single lognormal strokes are acting along a pivot, it can be seen that the angular variation is proportional to the traveled distance along the trajectory (i.e., $\phi(t) \propto l(t)$). This property can be used to estimate the angular parameters.

Eq. (33) shows the expression of the trajectory length as a function of time. Using Eqs. (18) and (33), the distance of p_i from the beginning of the movement is obtained as shown by Eq. (34):

$$l(t-t_0; D, \mu, \sigma) = \frac{D}{2}\left[1 + erf\left(\frac{\ln(t-t_0)-\mu}{\sigma\sqrt{2}}\right)\right] \tag{33}$$

$$l(t_i) = \begin{cases} 0 & \{i=1\} \\ \frac{D}{2}\left[1 + erf\left(\frac{-a_i}{\sigma\sqrt{2}}\right)\right] & \{i=2,3,4\} \\ D & \{i=5\} \end{cases} \tag{34}$$

Given the value of $\varphi_{\_n}(t_{i\_n})$ taken from $(x,y)_{\_n}$ and the values of $l(t_i)$ computed from the estimated values of σ and D, the angular parameters can be obtained by linear extrapolation using Eqs. (35) and (36):

$$\Delta\phi = \frac{\phi_{\_n}(t_{4\_n}) - \phi_{\_n}(t_{2\_n})}{l(t_4) - l(t_2)} \tag{35}$$

$$\theta_s = \phi_{\_n}(t_{3\_n}) - \Delta\phi(l(t_3) - l(t_1)) \tag{36a}$$

$$\theta_e = \phi_{\_n}(t_{3\_n}) - \Delta\phi(l(t_5) - l(t_3)) \tag{36b}$$

Furthermore, the angular parameters can be obtained in an analogous way using only two points from $\{p_2, p_3, p_4\}$ if one of these points is suspected to be less reliable than the others because of noise or important superposition of lognormal strokes.

3.7. Termination conditions

3.7.1. First mode

The first mode of extraction exits when no more valid characteristic point series are available for estimation (see Section 3.3) or

when the maximal amount of lognormal equation is reached. This latter condition is calculated such that the quantity of lognormal parameter used for reconstruction never exceeds the number of samples in the recorded movement.

3.7.2. Second mode

This mode terminates its execution for the same reasons than the first mode or if the total SNR is at least equal to the *SNRmin* value stated in Algorithm 1 or if adding a new stroke cause the SNR to drop 5 dB below the maximal value attained so far.

3.8. Optimization

3.8.1. Local optimization

Local optimization is performed after each lognormal estimation. This process is important because an inaccurate extraction of a lognormal will adversely affect the extraction of the following ones. The lsqnonlin Matlab function is used to non-linearly optimize four parameters μ, σ, θ_s, and θ_e. The other parameters (i.e., t_0 and D) are calculated in order to make the estimated lognormal maximum point equal to numerical maximum point (i.e., $p_{3\_a} = p_{3\_n}$).

3.8.2. Global optimization

After the extraction process is terminated, a final global optimization is performed to try to enhance the initial results. This is also done with the lsqnonlin Matlab function but it is performed in two iterations of three subsequent phases: velocity optimization (i.e., only t_0, D, μ, σ), angular optimization (i.e., only θ_s, θ_e), and full optimization (i.e., t_0, D, μ, σ, θ_s, θ_e). The velocity and the full optimization steps aim at minimizing the velocity error and therefore use the cost function (37), while the goal of the angular optimization is to minimize the error in the trace reconstruction and thus uses Eq. (38) as cost function:

$$f = (v_{x\_a} - v_{x\_n})^2 + (v_{y\_a} - v_{y\_n})^2 \tag{37}$$

$$f = (x_a - x_n)^2 + (y_a - y_n)^2 \tag{38}$$

Since the last optimization step performed is velocity oriented, the final trace (i.e., the X–Y plot) may suffer some offsets. However, since the Sigma–Lognormal model uses velocity, it seemed more useful to reduce velocity errors to get a maximum accuracy of the model parameters.

4. Results on signatures

4.1. Extraction performance evaluation

Extraction performances can be evaluated in many different ways but results are expected to have two principal characteristics: (1) the reconstruction error should be small and (2) the extracted solutions should be somehow consistent. In the following, for short, these two characteristics will be respectively referred as the fitness quality and the extraction consistency.

4.1.1. Fitness quality evaluation method

The first characteristic can be easily evaluated using the SNR between the reconstructed specimen and the original one. This measure has been chosen over the mean squared error to quantify the fitting accuracy because the latter is not normalized and therefore does not provide any comparative values between different signatures.

Various signals could be chosen for SNR calculation. Position signals are not adequate for this purpose for many reasons, the more important being that the signatures size has an impact on the SNR value. With such a signal, large fitting offsets far from the origin will have the same effect than smaller offsets happening closer to the origin. Velocity signals do not have this problem and are well suited for SNR calculation. To capture the effect of the distortions in both dimensions, a combination of Cartesian signals can be used. This results in the SNR_{vxy} definition given in Eq. (39):

$$SNR_{vxy} = 20 \log \left(\frac{\int_{t_s}^{t_e} [v_{x\_n}^2(t) + v_{y\_n}^2(t)]\,\mathrm{d}t}{\int_{t_s}^{t_e} [(v_{x\_n}(t) - v_{x\_a}(t))^2 + (v_{y\_n}(t) - v_{y\_a}(t))^2]\,\mathrm{d}t} \right) \tag{39}$$

While SNR based on tangential speed, as shown in Eq. (40), is perfectly adequate when working with the one-dimensional Delta–Lognormal model, this formulation should be avoided when working with Sigma–Lognormal model because it do not take in account the vectorial nature of the tangential velocity:

$$SNR_{vt} = 20 \log \left(\frac{\int_{t_s}^{t_e} v_{t\_n}^2(t)\,\mathrm{d}t}{\int_{t_s}^{t_e} (v_{t\_n}(t) - v_{t\_a}(t))^2\,\mathrm{d}t} \right) \tag{40}$$

4.1.2. Extraction consistency evaluation method

To evaluate the consistency of the extracted results, without designing a full verification system, is a difficult task but a few heuristics may be used. The first one of these is the analysis of the number of lognormal equations used in the reconstruction. For a given SNR, as obtained from the fitting of a particular specimen, a smaller number of lognormal strokes is generally better. Moreover, for a stable signee, this number should have a small variability from specimen to specimen.

A second heuristic is based on virtual targets [25]. These are defined as final positions that would have been reached by isolated lognormals. Virtual targets are connected together though virtual trajectories which are also obtained by removing lognormals stroke interactions. These targets and trajectories can be used to study the correspondence between the extraction results and what is thought to be the underlying process that generated the original data, i.e., "does the extracted solution form a plausible action plan for the movement realized?"

Finally, the third heuristic considered is the analysis of the accordance between the extraction results and the Sigma–Lognormal model-based knowledge acquired from the kinematics theory of rapid human movements [53,73].

4.2. Signature databases description

The extractor has been tested on two databases. The first one is a proprietary database containing 683 signatures obtained from 124 subjects. It contains 4 to 8 specimens of each class. The signatures were digitized at 200 Hz using a Wacom Intuos tablet.

The second database is the publicly available SVC2004 database [81]. It is separated in two subsets (task 1 and 2) of 1600 specimens. Each subset contains 40 different classes constituted of 20 genuine signatures and 20 skilled forgeries. Subjects were suggested to design a new signature especially for these acquisitions instead of using their real one. Data collection was conducted at 100 Hz with Wacom tablets.

4.3. Extraction results

4.3.1. Fitness quality evaluation

The entire extraction process was completely automated. No manual preprocessing of any kind has been conducted on data. Fig. 4 shows histograms of extraction SNR_{vxy} obtained. Table 4 also gives principal statistics of the reconstruction accuracy. Some examples of reconstruction are shown in Fig. 5. On these plots, the continuous

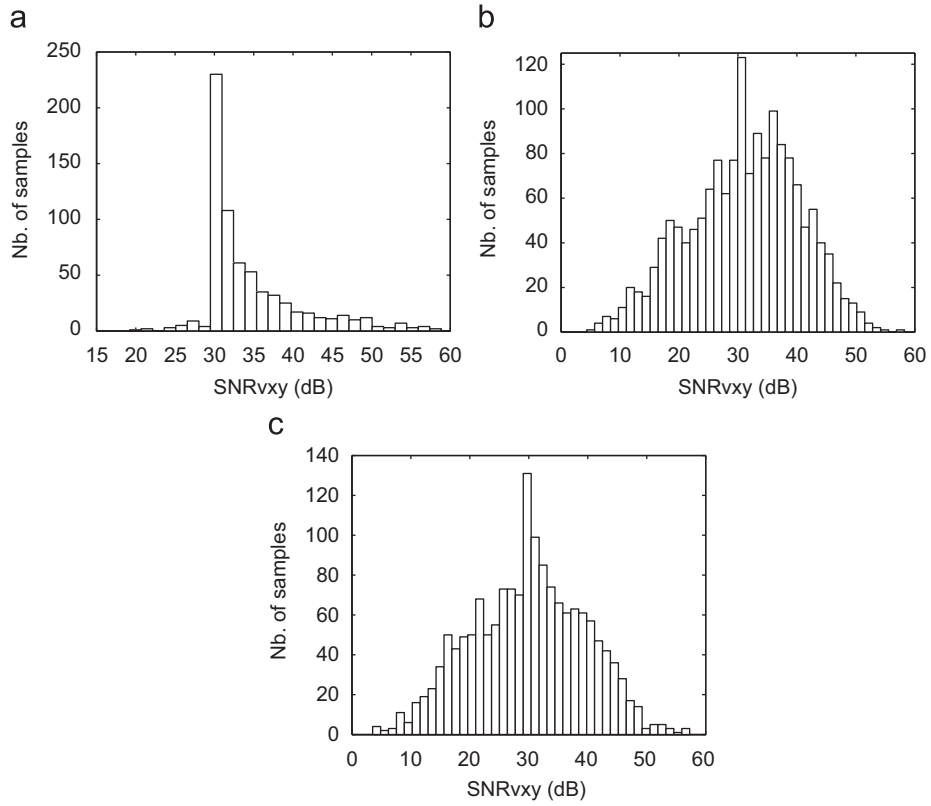

Fig. 4. Histograms of reconstruction SNR obtained on (a) the proprietary database and the SVC2004 database for (b) task 1 and (c) task 2.

Table 4
SNR_{vxy} obtained with extracted parameters (in dB)

Database	Mean	Standard deviation	Minimum	Maximum
Proprietary	34.7	6.3	19.2	58.9
SVC2004—task 1	31.1	9.4	4.3	58.2
SVC2004—task 2	29.9	9.6	3.5	57.3

lines shows the original signature traces (a, c, e) and their velocity magnitude (b, d, f). The dashed lines depict the results obtained from the $\Sigma\Lambda$ synthesis from the extracted parameters. Table 5 gives the corresponding extraction characteristics.

Since a SNR greater than 30 dB is considered to be sufficient [78] in human movement analysis, results on our proprietary database are quite satisfactory. Results on the SV2004 database, although acceptable, are a little less satisfactory. As depicted in Table 4, their averaged SNR is lower and have a greater standard deviation. Furthermore, Fig. 4 shows that while there is almost no extraction below the 30 dB threshold for the extractions on our proprietary database, this is not the case with results on SVC2004. Some reasons may be hypothesized to explain this performance drop such as a lower sampling rate—100 Hz instead of 200 Hz—and a non-zero velocity signal truncation. Fig. 6 gives an example of a 13.0 dB extraction illustrating the impact of the latter cause, a signature where the subject has removed the pen out of the sensitive area of the digitizer prior to finishing the signing process. It shows that the missing speed signal at the end results in the absence of the corresponding strokes in estimation. The global optimization step has the effect of distorting the signal to compensate for this omission, degrading further the solution. A preprocessing step cutting the signal at the local minimum immediately preceding a non-zero velocity signal at the end could help on this kind of data. The application of such treatment on the example of Fig. 6 resulted in a 40 dB extraction.

4.3.2. Analysis of extraction consistency

Regarding the first heuristic for analyzing the extraction consistency, the intra-class standard deviation of the number of extracted lognormal stroke is about 10%. This means a deviation of more or less one stroke for every 10 strokes. Such variability seems acceptable given the normal variability of signatures and the lack of manual preprocessing on the data to ensure an accurate truncation of artifacts before and after the signatures.

An average of 14.2 lognormal strokes for the reconstruction of the signatures from the class shown in Figs. 5a and b has been obtained. This number is a great improvement over previously published results which gave a mean of 38.3 strokes [80]. Also, as expected, this corresponds approximately to the number of distinguishable local maxima. An inexact correspondence is acceptable, since lognormal strokes can be hidden in the tangential velocity profiles in such way that they do not produce an observable local maximum. However, the amount of such hidden strokes should be relatively low with respect to the number of visible ones.

Visual inspection of results from Sigma–Lognormal reconstruction of movement signals reveals some interesting points regarding the second heuristic. On high quality extraction (i.e., high SNR and adequate number of lognormal stroke), a highly plausible virtual trajectory is obtained as shown in Fig. 7a and b. A less plausible result is identified by "B" arrows in Fig. 7c and d. These strokes show a virtual trajectory far less in accordance with the movement performed. Moreover, such virtual trajectory would require a high level of muscular co-contraction and thus results in poor movement efficiency. Parsimony and efficiency suggest that strokes identified by "B" arrows are probably not revealing the true nature of the underlying process that generated the final movement.

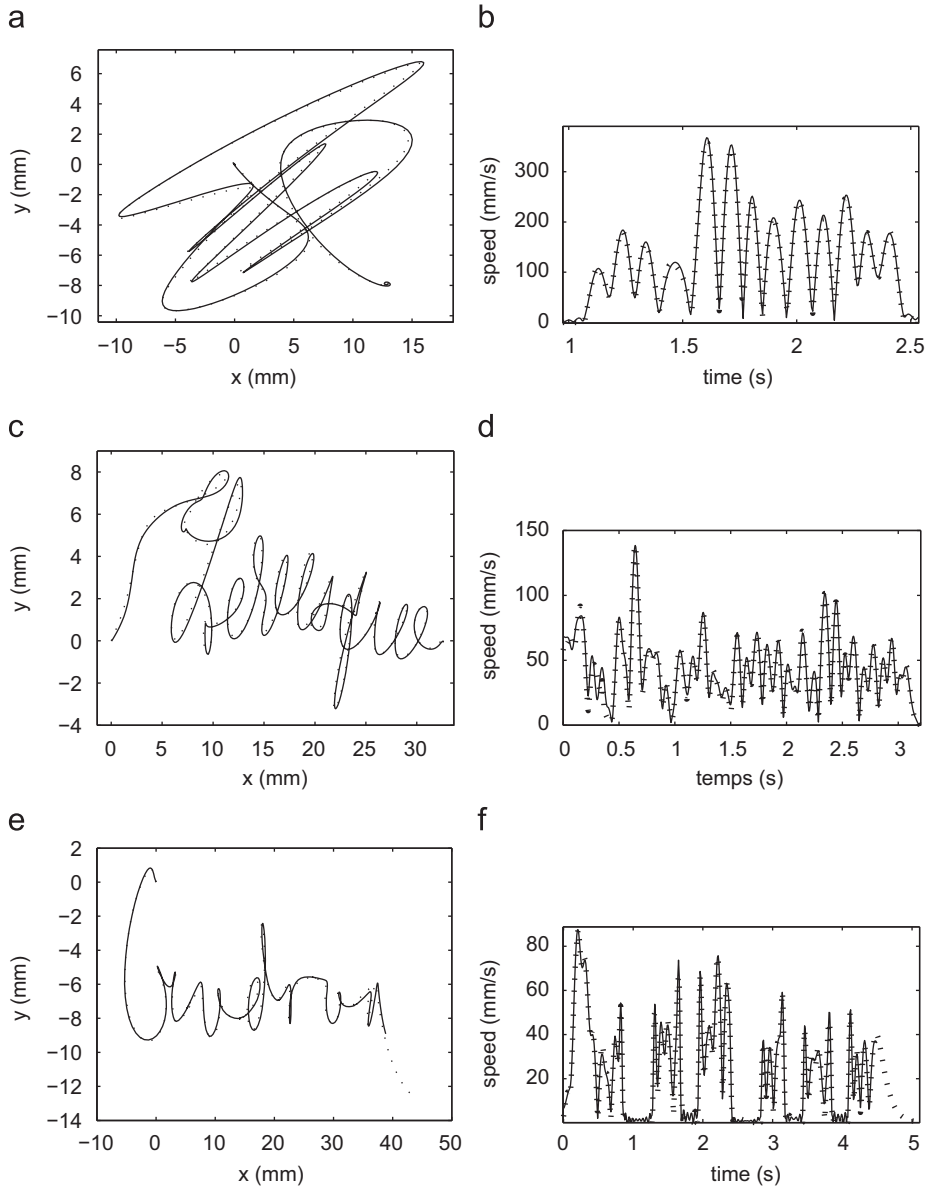

Fig. 5. Signature reconstruction from the extracted parameters. Plot (a–d) are from our proprietary database, while plots (e and f) is from specimen U12S1 from SVC2004 (task 1) database.

Table 5
Extraction results characteristics for plots shown in Fig. 5

Plot	SNR_{vxy} (dB)	No. of lognormal extracted
5a and b	56.3	15
5c and d	37.3	39
5e and f	39.4	40

Concerning the third heuristic, the "A" arrows in Figs. 7a–d shows an example of utilization of model-based knowledge applied to the analysis of extraction results. They point out that the extractor uses an antagonist lognormal to model signature's sharp ending. This behavior was not specifically intended in the extractor development. It can be seen from Fig. 7e that when the ending is truncated, as it is unfortunately often the case in the SVC2004 database, the algorithm cannot predict the movement ending. Therefore, it does not add a final antagonist lognormal to terminate the movement sharply and thus the movement slowly fades out. Interestingly, the antagonist stroke at the end of a sharp movement appeared to be a natural characteristic emerging when good quality extraction are obtained, as predicted by the kinematics theory of rapid human movements [53,73].

5. Conclusion and future works

In this paper, the development of a completely automatic parameter extractor able to devise a signature representation based on the $\Sigma\Lambda$ model has been presented. To our knowledge, it is the first robust extractor developed for such a purpose. It availability should provide new possibilities not only for the analysis of large databases of signatures but also for the analysis of complex human movements such as those used in biomedical studies.

The proposed kind of modeling solves many online signature preprocessing and representation problems still challenging [82]. Indeed, processes such as segmentation and feature extraction are embedded in the extraction of the $\Sigma\Lambda$ parameters. Moreover, the

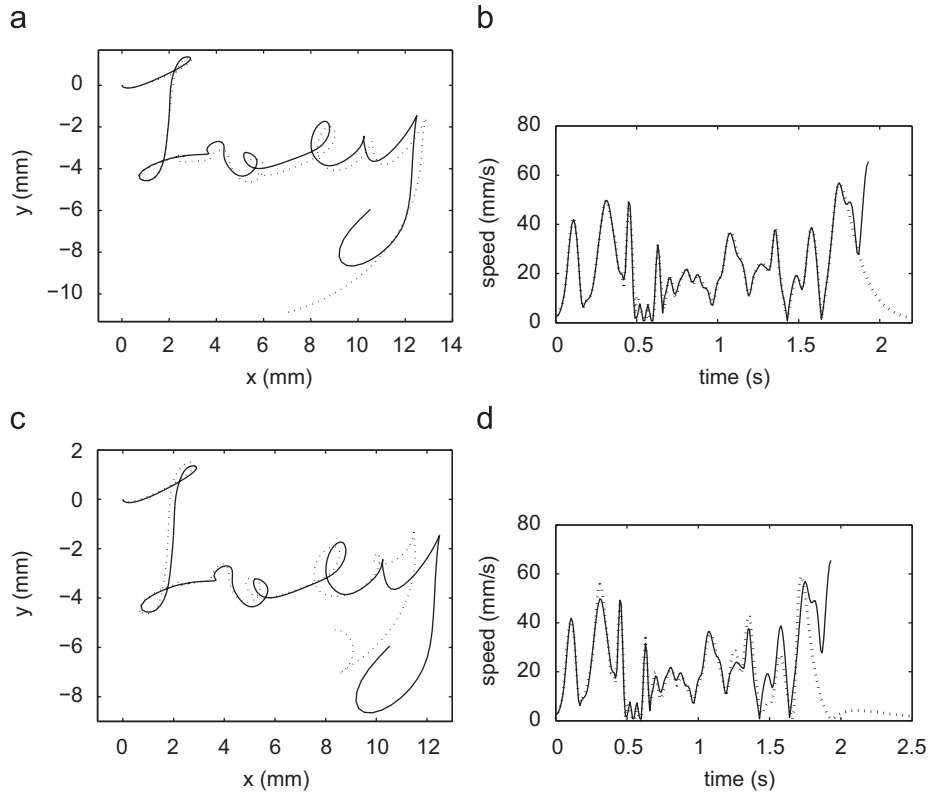

Fig. 6. Illustration of reconstruction for a low SNR extraction (SVC2004—task 2-U10S22). Solid lines are original signals, dot lines are reconstruction. Plots (a and b) and (c and d) shows, respectively, results before and after the global optimization.

examination of the variability of these parameters can already be used in many applications such as signature stability analysis, signatures or handwritten characters database generation, signee characterization, study of the signature evolution through time or of the effect of aging, etc.

At this moment, the verification of signatures is not at reach. The work presented here is a first step aiming at modeling signature by lognormals. The principal goals here were to obtain extractions laying satisfactory fittings and forming plausible action plans. We also wanted to provide some evaluation criteria without designing a whole verification system. Work regarding class descriptions and samples similarity measurement has still to be conducted for signature verification to be performed.

Finally, although the performances reported in Fig. 5 look quite impressive, there is still room for improvements. In order to reach a sufficient level of accuracy, robustness and flexibility for commercial and industrial requirements, research efforts will have to be conducted on various topics such as an in-depth study of $\Sigma\Lambda$ parameter variability, and the development of a reliable quantitative measure of the intra-class extraction consistency.

Acknowledgments

This work was partly supported by NSERC Grant RGPIN-915 to Réjean Plamondon. The proprietary database was collected during a research project supported by the Fondation Lucie and André Chagnon.

Appendix A

Table 6 describes the mathematical notation used throughout the text.

Appendix B

A direct expression for $x(t;P)$ such as shown in Eq. (41) can be computed as follows. The development is given only for $x(t;P)$, the steps to obtain $y(t;P)$ being similar:

$$\begin{aligned} x(t;P) &= \int_0^t v_x(\tau;P)\,\mathrm{d}\tau \\ &= \int_0^t \sum_{j=1}^{M} |\vec{v}_j(\tau;P_j)|\,\cos(\phi_j(\tau;P_j))\,\mathrm{d}\tau \\ &= \sum_{j=1}^{M} x_j(\tau;P_j) \end{aligned} \tag{41}$$

From the hypothesis that every lognormal stroke are acting along a pivot, it can be said that $(x_j(\tau;P_j), y_j(\tau;P_j))$ form a circular trajectory with a radius given by $r = D_j/|\Delta\theta_j|$ where $\Delta\theta_j = \theta_e - \theta_s$. This curve can be parameterized for the abscissa as given by Eq. (42):

$$x_j(\tau;P_j) = r\,\cos(m(\tau;P_j)) \tag{42}$$

Since this curve has to start at a θ_{sj} angle, it must be transformed as shown in Fig. 8.

The corresponding parameterization has to be updated as in Eq. (43) where x_0 is given by Eq. (44):

$$x_j(\tau;P_j) = \frac{D_j}{|\Delta\theta_j|}\cos(m(\tau;P_j)) - x_0 \tag{43}$$

$$x_0 = \frac{D_j}{|\Delta\theta_j|}\cos(\theta_j) \tag{44}$$

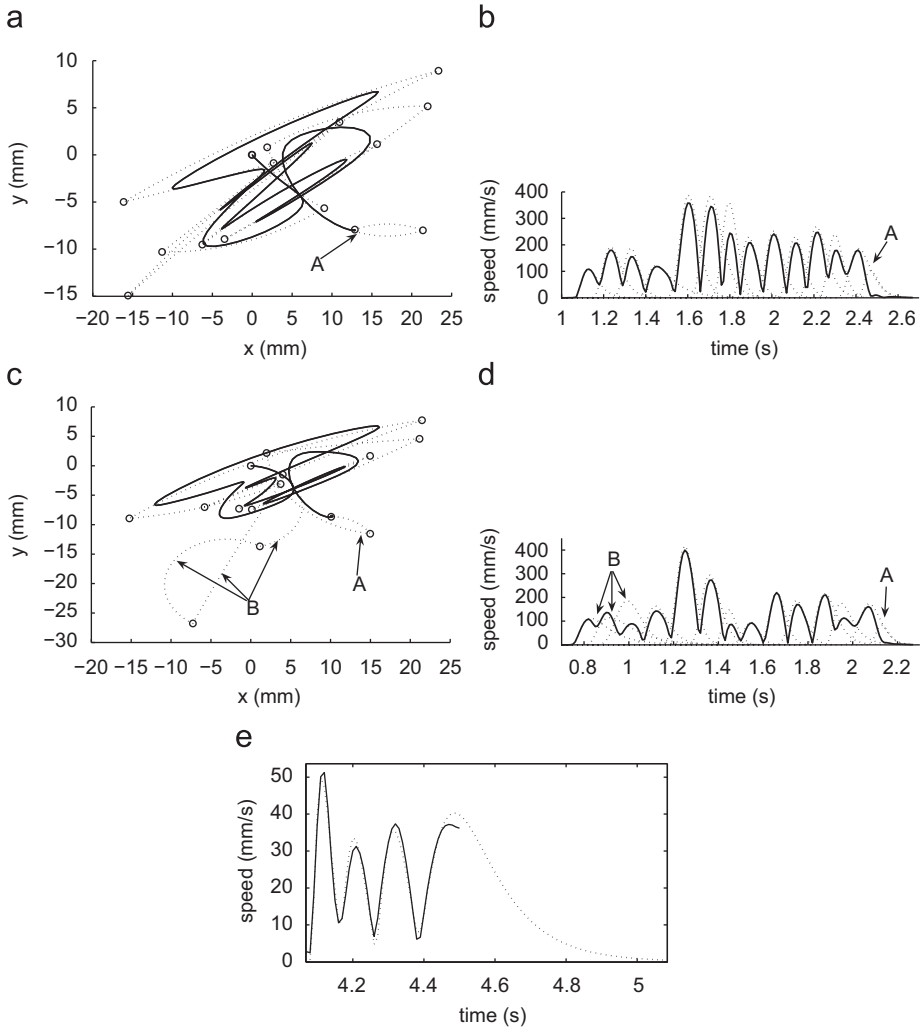

Fig. 7. (a and c) Virtual trajectory (dotted line) compared to extracted trajectory (strong line) with their (d and e) corresponding velocity profile (strong line) and it decomposition in lognormal stroke (dotted line). (e) Illustration of the absence of antagonist stroke when signal's ending is severely truncated at a non-zero velocity.

Table 6
Mathematical notation used

Symbol	Meaning	Indices possibly taken
$\|\dots\|$	Modulus operator	N/A
$\rightarrow$ (over a symbol)	Indicates a vectorial signal	N/A
$\bullet$ (over a symbol)	Time derivative operator	N/A
t (as exponent)	Matrix transposition operator	N/A
v_t	Tangential speed	i,j,_n,_a
t_i	Time	i,j,_n,_a
P	Sigma–Lognormal parameter matrix	J
x, y	Cartesian position	i,j,_n,_a
v_x, v_y	Cartesian speed	i,_n,_a
D, t_0, μ, σ, θ_s, θ_e	Sigma–Lognormal parameters	J
p_i	Lognormal characteristic point constituted of two coordinates (t_i, v_{ti})	I
φ	Angular position signal	j,_n,_a
l	Traveled distance (i.e., integration of tangential speed)	j,_n,_a
i (as index)	Indices of a lognormal characteristic point	N/A
j (as index)	Indicates that only the jth stroke is considered	N/A
_n (as index suffix)	Indicates that the value is taken from the numerical signal	N/A
_a (as index suffix)	Indicates that the value is taken from the analytical signal synthesized from Sigma–Lognormal parameters	N/A

The m parameter is time dependent and may be expressed as a function of the traveled distance $l(t; P_j)$ as shown in Eq. (45):

$$m(\tau; P_j) = \theta_i + \Delta\theta_j \frac{l(\tau; P_j)}{D_j} \tag{45}$$

However, θ_i still has to be expressed as a Sigma–Lognormal parameter. As can be seen in Fig. 9, θ_i may be expressed relatively as θ_{sj} differently whether the rotation is clockwise (i.e., $\Delta\theta_j > 0$) or anti-clockwise (i.e., $\Delta\theta_j < 0$). This is expressed

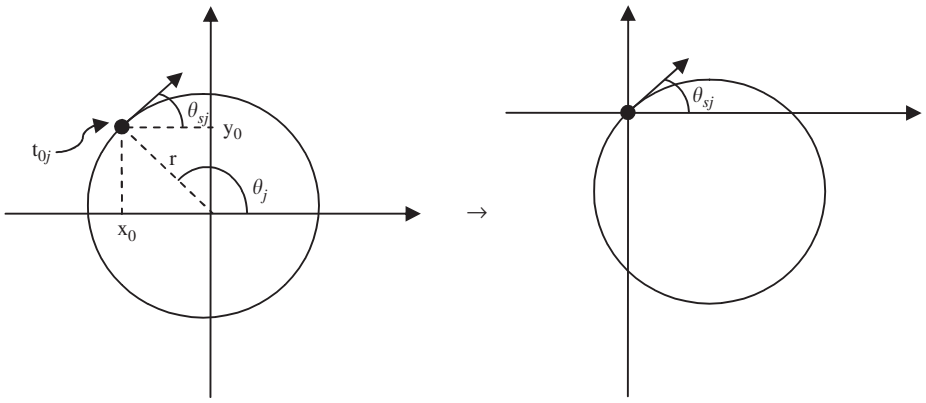

Fig. 8. Origin translation for curve parameterization.

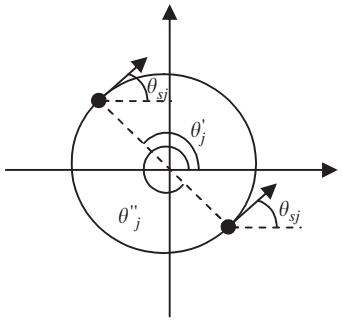

Fig. 9. Illustration of the $\theta_i - \theta_{sj}$ correspondence.

in Eq. (46):

$$\theta_j = \begin{cases} \theta''_j = \theta_{sj} + \dfrac{\pi}{2} & \text{if } \Delta\theta_j \leqslant 0 \\ \theta'_j = \theta_{sj} - \dfrac{\pi}{2} & \text{if } \Delta\theta_j > 0 \end{cases} = \theta_{sj} - \frac{\Delta\theta_j}{|\Delta\theta_j|}\frac{\pi}{2} \tag{46}$$

Therefore, Eq. (43) can be stated as in Eq. (47):

$$x_j(t;P_j) = \frac{Dj}{|\Delta\theta_j|}\left[\cos\left(\theta_{sj} - \frac{\Delta\theta_j}{|\Delta\theta_j|}\frac{\pi}{2} + \Delta\theta_j\frac{l_j(t;P_j)}{D_j}\right) - \cos\left(\theta_{sj} - \frac{\Delta\theta_j}{|\Delta\theta_j|}\frac{\pi}{2}\right)\right] \tag{47}$$

Moreover, since $\cos(\alpha \pm \pi/2) = \pm\sin(\alpha)$, (47) may be expressed as in Eq. (48):

$$x_j(t;P_j) = \frac{Dj}{\Delta\theta_j}\left[\sin\left(\theta_{sj} + \Delta\theta_j\frac{l_j(t;P_j)}{D_j}\right) - \sin(\theta_{sj})\right] \tag{48}$$

Considering the expression of $l(t;P_j)$ as given by Eq. (49), the single stroke equation of the Cartesian abscissa can be expressed in the elegant form given by Eq. (50):

$$l_j(t;P_j) = D_j\frac{\phi_j(t;P_j) - \theta_{sj}}{\Delta\theta_j} \tag{49}$$

$$x_j(t;P_j) = \frac{D_j}{\Delta\theta_j}[\sin(\phi_j(t;P_j)) - \sin(\theta_{sj})] \tag{50}$$

We finally obtain (11) with $\phi_j(t;P_j)$ as given in Eq. (2). Eq. (12) is obtained by a similar development. However, it should be noted that these equations are singular for a strait movement. Therefore, as $r \to \infty$, it should be replaced by the linear estimation (51):

$$x_j(t;P_j) = l_j(t;P_j)\cos(\theta_{sj}) \tag{51}$$

References

[1] F. Leclerc, R. Plamondon, Automatic signature verification: the state of the art 1989–1993, Int. J. Pattern Recognition Artif. Intell. 8 (3) (1994) 643–659.
[2] J. Fierrez, J. Ortega-Garcia, Function-based online signature verification, in: N.K. Ratha, V. Govindaraju (Eds.), Advances in Biometrics, Springer, London, 2008, pp. 225–245.
[3] G. Dimauro, et al., Analysis of stability in hand-written dynamic signatures, in: Proceedings of the Eighth International Workshop on Frontiers in Handwriting Recognition, 2002, pp. 259–263.
[4] B. Kar, P.K. Dutta, T.K. Basu, C.V. Hauer, J. Dittmann, DTW based verification scheme of biometric signatures, in: IEEE International Conference on Industrial Technology, 2006, pp. 381–386.
[5] H. Feng, C. Choong Wah, Online signature verification using a new extreme points warping technique, Pattern Recognition Letters 24 (16) (2003) 2943–2951.
[6] Y. Sato, K. Kogure, Online signature verification based on shape, motion, and writing pressure, in: Proceedings of the Sixth International Conference on Pattern Recognition, 1982, pp. 823–826.
[7] M. Yasuharam, M. Oka, Signature verification experiment based on nonlinear time alignment: a feasibility study, IEEE Trans. Syst. Man Cybern. 7 (3) (1977) 212–216.
[8] M. Parizeau, R. Plamondon, A comparative analysis of regional correlation, dynamic time warping, and skeletal tree matching for signature verification, IEEE Trans. Pattern Anal. Mach. Intell. 12 (7) (1990) 710–717.
[9] R. Martens, L. Claesen, On-line signature verification by dynamic time-warping, in: Proceedings of the 13th International Conference on Pattern Recognition, vol. 3, 1996, pp. 38–42.
[10] M. E. Munich, P. Perona, Continuous dynamic time warping for translation-invariant curve alignment with applications to signature verification, in: The Seventh International Conference on Computer Vision, vol. 1, 1999, pp. 108–115.
[11] B. Wirtz, Stroke-based time warping for signature verification, in: Proceedings of the Third International Conference on Document Analysis and Recognition, vol. 1, 1995, pp. 179–182.
[12] K. Huang, H. Yan, On-line signature verification based on dynamic segmentation and global and local matching, Opt. Eng. 34 (12) (1995) 3480–3487.
[13] V.S. Nalwa, Automatic on-line signature verification, Proc. IEEE 85 (2) (1997).
[14] R. Martens, L. Claesen, Dynamic programming optimisation for on-line signature verification, in: Proceedings of the Fourth International Conference on Document Analysis and Recognition, vol. 2, 1997, pp. 653–656.
[15] T. Hastie, E. Kishon, M. Clark, J. Fan, A model for signature verification, in: Proceedings of the IEEE International Conference on Systems, Man, and Cybernetics, vol. 1, 1991, pp. 191–196.
[16] M.K. Khan, M.A. Khan, M.A.U. Khan, S. Lee, Signature verification using velocity-based directional filter bank, in: IEEE Asia Pacific Conference on IEEE Asia Pacific Conference on Circuits and Systems, 2006, pp. 231–234.
[17] K. Huang, H. Yan, Stability and style-variation modeling for on-line signature verification, Pattern Recognition 36 (10) (2003) 2253–2270.
[18] C. Rabasse, R.M. Guest, M.C. Fairhurst, A new method for the synthesis of signature data with natural variability, IEEE Trans. Syst. Man Cybern. B 38 (3) (2008) 691–699.
[19] M. Wirotius, J.Y. Ramel, N. Vincent, Distance and matching for authentication by on-line signature, in: Fourth IEEE Workshop on Automatic Identification Advanced Technologies, 2005, pp. 230–235.

[20] D.S. Guru, H.N. Prakash, Symbolic representation of on-line signatures, in: Proceedings of the International Conference on Computational Intelligence and Multimedia Applications, vol. 2, 2007, pp. 312–317.
[21] F. Bauer, B. Wirtz, Parameter reduction and personalized parameter selection for automatic signature verification, in: Proceedings of the Third International Conference on Document Analysis and Recognition, vol. 1, 1995, pp. 183–186.
[22] S.H. Kim, M.S. Park, J. Kim, Applying personalized weights to a feature set for on-line signature verification, in: Proceedings of the Third International Conference on Document Analysis and Recognition, vol. 2, 1995, pp. 882–885.
[23] L.L. Lee, T. Berger, E. Aviczer, Reliable on-line human signature verification systems, IEEE Trans. Pattern Anal. Mach. Intell. 18 (6) (1996) 643–647.
[24] R. Plamondon, G. Lorette, Automatic signature verification and writer identification—the state of the art, Pattern Recognition 22 (2) (1989) 107–131.
[25] R. Plamondon, S.N. Srihari, Online and off-line handwriting recognition: a comprehensive survey, IEEE Trans. Pattern Anal. Mach. Intell. 22 (1) (2000) 63–84.
[26] L. Yang, B.K. Winjaja, R. Prasad, Application of hidden markov models for signature verification, Pattern Recognition 28 (2) (1995) 161–170.
[27] R.S. Kashi, J. Hu, W.L. Nelson, W. Turin, On-line handwritten signature verification using hidden Markov model features, in: Proceedings of the Fourth International Conference on Document Analysis and Recognition, vol. 1, 1997, pp. 253–257.
[28] J.G.A. Dolfing, E.H.L. Aarts, J.J.G.M. van Oosterhout, On-line signature verification with hidden Markov models, in: Proceedings of the Fourteenth International Conference on Pattern Recognition, vol. 2, 1998, pp. 1309–1312.
[29] J. Fierrez, J. Ortega-Garcia, D. Ramosa, J. Gonzalez-Rodrigueza, HMM-based on-line signature verification: Feature extraction and signature modeling, Pattern Recognition Lett. 28 (16) (2007) 2325–2334.
[30] G. Rigoll, A. Kosmala, A systematic comparison between on-line and off-line methods for signature verification with hidden Markov models, in: Proceedings of the Fourteenth International Conference on Pattern Recognition, vol. 2, 1998, pp. 1755–1757.
[31] M.J. Paulik, N. Mohankrishnan, A 1-D, sequence decomposition based, autoregressive hidden Markov model for dynamic signature identification and verification, in: Proceedings of the 36th Midwest Symposium on Circuits and Systems, vol. 1, 1993.
[32] M. Fuentes, S. Garcia-Salicetti, B. Dorizzi, On line signature verification: fusion of a hidden Markov model and a neural network via a support vector machine, in: Proceedings of the Eighth International Workshop on Frontiers in Handwriting Recognition, 2002, pp. 253–258.
[33] D. Muramatsu, T. Matsumoto, An HMM online signature verifier incorporating signature trajectories, in: Proceedings of the Seventh International Conference on Document Analysis and Recognition, vol. 1, 2003, pp. 438–442.
[34] H.S. Yoon, J.Y. Lee, H.S. Yang, An online signature verification system using hidden Markov model in polar space, in: Proceedings of the Eighth International Workshop on Frontiers in Handwriting Recognition, 2002, pp. 329–333.
[35] J.G.A. Dolfing, E.H.L. Aarts, J.J.G.M. van Oosterhout, On-line verification signature with hidden Markov models, in: Proceedings of the 14th International Conference Pattern Recognition, 1998, pp. 1309–1312.
[36] D. Muramatsu, T. Matsumoto, An HMM on-line signature verifier incorporating signature trajectories, in: Proceedings of the Seventh International Conference on Document Analysis and Recognition, vol. 1, 2003, pp. 438–442.
[37] R.S. Kashi, J. Hu, W.L. Nelson, W. Turin, A hidden Markov model approach to online handwritten signature verification, Int. J. Doc. Anal. Recognition 1 (2) (1998) 102–109.
[38] J. Tianshi, Z. Changshui, Signature data generation method, in: SPIE Proceedings Series, vol. 4553, 2001, pp. 338–347.
[39] D.C.L. Kamins, K. Zimmermann, Signature recognition through spectral analysis, in: IEEE International Conference on Acoustics, Speech, and Signal Processing, vol. 12, 1987, pp. 1790–1792.
[40] M. Mingming, W.S. Wijesona, Automatic on-line signature verification based on multiple models, in: Proceedings of the Conference on Computational Intelligence for Financial Engineering, 2000, pp. 30–33.
[41] C.S. Sundaresan, S.S. Keerthi, A study of representations for pen based handwriting recognition of Tamil characters, in: Proceedings of the Fifth International Conference on Document Analysis and Recognition, 1999, pp. 422–425.
[42] A.V. Da Silva, D.S. De Freitas, Wavelet-based compared to function-based on-line signature verification, in: Proceedings of the XV Brazilian Symposium on Computer Graphics and Image, 2002, pp. 218–225.
[43] J. Richiardi, H. Ketabdar, A. Drygajlo, Local and global feature selection for on-line signature verification, in: Proceedings of the Eighth International Conference on Document Analysis and Recognition, vol. 2, 2005, pp. 625–629.
[44] M. Mingming, W.S. Wijesoma, E. Sung, An automatic on-line signature verification system based on three models, in: Canadian Conference on Electrical and Computer Engineering, vol. 2, 2000, pp. 890–894.
[45] T.H. Rhee, S.J. Cho, J.H. Kim, On-line signature verification using model-guided segmentation and discriminative feature selection for skilled forgeries, in: Proceedings of the Sixth International Conference on Document Analysis and Recognition, 2001, pp. 645–649.
[46] T. Qu, A. El Saddik, A. Adler, Dynamic signature verification system using stroked based features, in: Proceedings of the second IEEE International Workshop on Haptic, Audio and Visual Environments and Their Applications, 2003, pp. 83–88.
[47] L. Nanni, Experimental comparison of one-class classifiers for online signature verification, Neurocomputing 69 (7–9) (2006) 869–873.
[48] K.W. Yue, W.S. Wijesoma, Improved segmentation and segment association for on-line signature verification, in: IEEE International Conference on Systems, Man, and Cybernetics, vol. 4, 2000, pp. 2752–2756.
[49] C. Schmidt, K.-F. Kraiss, Establishment of personalized templates for automatic signature verification, in: Proceedings of the Fourth International Conference on Document Analysis and Recognition, vol. 1, 1997, pp. 263–267.
[50] M.A. Alimi, Beta neuro-fuzzy systems, in: W. Duch, D. Rutkowska (Eds.), TASK Quarterly J., Special Issue on Neural Networks, vol. 7(1), 2003, pp. 23–41.
[51] N. Hogan, An organization principle for a class of voluntary movements, J. Neurosci. 4 (1984) 2745–2754.
[52] W.L. Nelson, Physical principles for economies of skilled movements, Biol. Cybern. 46 (1983) 135–147.
[53] R. Plamondon, A kinematic theory of rapid human movements. I. Movement representation and generation, Biol. Cybern. 72 (4) (1995) 295–307.
[54] D. Bullock, S. Grossberg, The VITE model: a neural command circuit for generating arm and articulator trajectories, in: J.A.S. Kelso, A.J. Mandell, M.F. Shlesinger (Eds.), Dynamic Patterns in Complex Systems, World Scientific Publishers, Singapore, 1988, pp. 305–326.
[55] C.M. Harris, D.M. Wolpert, Signal-dependent noise determines motor planning, Nature 394 (1998) 780–784.
[56] P.D. Neilson, The problem of redundancy in movement control: the adaptive model theory approach, Psychol. Res. 55 (1993) 99–106.
[57] P.D. Neilson, M.D. Neilson, An overview of adaptive model theory: solving the problems of redundancy, resources and nonlinear interactions in human movement control, J. Neural Eng. 2 (3) (2005) 279–312.
[58] H. Tanaka, J.W. Krakauer, N. Qian, An optimization principle for determining movement duration, J. Neurophysiol. 95 (2006) 3875–3886.
[59] Y. Uno, M. Kawato, R. Suzuki Formation, Control of optimal trajectory in human multijoint arm movement, Biol. Cybern. 61 (1989) 89–101.
[60] G. Gangadhar, D. Joseph, V.S. Chakravarthy, An oscillatory neuromotor model of handwriting generation, Int. J. Doc. Anal. Recognition 10 (2) (2007) 69–84.
[61] A.G. Feldman, M.L. Latash, Testing hypotheses and the advancement of science: recent attempts to falsify the equilibrium point hypothesis, Exp. Brain Res. 161 (1) (2005) 91–103.
[62] E. Bizzi, N. Hogan, F.A. Mussa-Ivaldi, S. Giszter, Does the nervous system use equilibrium-point control to guide single and multiple joint movements?, Behav. Brain Sci. 15 (1992) 603–613.
[63] S.E. Engelbrecht, Minimum principles in motor control, J. Math. Psychol. 45 (2001) 497–542.
[64] J.D. Enderle, J.W. Wolfe, Time-optimal control of saccadic eye movements, IEEE Trans. Biomed. Eng. 34 (1987) 43–55.
[65] P.D. Neilson, The problem of redundancy in movement control: the adaptive model theory approach, Psychol. Res. 55 (1993) 99–106.
[66] T. Flash, N. Hogan, The coordination of arm movements: an experimentally confirmed mathematical model, J. Neurosci. 5 (1985) 1688–1703.
[67] S. Edelman, T. Flash, A model of handwriting, Biol. Cybern. 57 (1987) 25–36.
[68] Y. Uno, R. Suzuki, M. Kawato, Formation and control of optimal trajectories in human multijoint arm movements, Biol. Cybern. 61 (1989) 89–101.
[69] J.M. Hollerbach, An oscillation theory of handwriting, Biol. Cybern. 39 (2) (1981) 139–156.
[70] G. Gangadhar, D. Joseph, V.S. Chakravarthy, An oscillatory neuromotor model of handwriting generation, Int. J. Doc. Anal. Recognition 10 (2) (2007) 69–84.
[71] L.R.B. Schomaker, Simulation and recognition of handwriting movement: a vertical approach to modeling human motor behavior, PhD Thesis, Nijmegen University, Netherlands, 1991.
[72] K.T. Kalveram, A neural oscillator model learning given trajectories, or how an allo-imitation algorithme can be implemented into a motor controller, in: J.P. Piek (Ed.), Motor Behavior and Human Skill: A Multidisciplinary Approach, Human Kinetics, 1998, pp. 127–140.
[73] R. Plamondon, A kinematic theory of rapid human movements. II. Movement time and control, Biol. Cybern. 72 (4) (1995) 309–320.
[74] S. Grossberg, R.W. Paine, A neural model of corticocerebellar interactions during attentive imitation and predictive learning of sequential handwriting movements, Neural Netw. 13 (2000) 999–1046.
[75] Y. Wada, M. Kawato, A theory for cursive handwriting based on the minimization principle, Biol. Cybern. 73 (1) (1995) 3–13.
[76] D.M. Wolpert, Z. Ghahramani, M.I. Jordan, Are arm trajectories planned in kinematic or dynamic coordinates? An adaptation study, Exp. Brain Res. 103 (3) (1995) 460–470.
[77] R. Plamondon, R.M. Parizeau, Signature verification from position, velocity and acceleration signals: a comparative study, in: The Ninth International Conference on Pattern Recognition, vol. 1, 1988, pp. 260–265.
[78] M. Djioua, R. Plamondon, A new algorithm and system for the extraction of delta-lognormal parameters, Technical Report EPM-RT-2008-04, École Polytechnique de Montréal, 2008.
[79] W. Guerfali, R. Plamondon, A new method for the analysis of simple and complex planar rapid movements, J. Neurosci. Methods 82 (1) (1998) 35–45.
[80] C. O'Reilly, R. Plamondon, Automatic extraction of sigma-lognormal parameters on signatures, in: Proceedings of the 11th International Conference on Frontier in Handwriting Recognition, to appear.
[81] D.-Y. Yeung, et al., SVC2004: first international signature verification competition, in: Proceedings of International Conference on Biometric Authentication (ICBA), Springer LNCS-3072, July 2004, pp. 16–22.
[82] G. Dimauro, et al. Recent advancements in automatic signature verification, in: Proceedings of the Ninth International Workshop on Frontiers in Handwriting Recognition, 2004, pp. 179–184.

About the Author—CHRISTIAN O'REILLY received B.Ing. in Electrical Engineering (2007) and is currently pursuing a Ph.D. degree in Biomedical Engineering at the École Polytechnique de Montréal.

About the Author—RÉJEAN PLAMONDON received a B.Sc. degree in Physics, and M.Sc.A. and Ph.D. degrees in Electrical Engineering from Université Laval, Québec, P.Q., Canada, in 1973, 1975, and 1978, respectively. In 1978, he joined the faculty of the École Polytechnique, Université de Montréal, Montréal, P.Q., Canada, where he is currently a Full Professor. He has been the Head of the Department of Electrical and Computer Engineering from 1996 to 1998 and the Chief Executive Officer of Ecole Polytechnique from 1998 to 2002. He is now the Head of Laboratoire Scribens at this institution.

Over the last 25 years, Professor Plamondon has been involved in many pattern recognition projects, particularly in the field of on-line and off-line handwriting analysis and processing. He has proposed many original solutions, based on exhaustive studies of human movements generation and perception, to problems related to the design of automatic systems for signature verification and handwriting recognition, as well as interactive electronic penpads to help children learn handwriting and powerful methods for analyzing and interpreting neuromuscular signals. His main contribution was the development of a kinematic theory of rapid human movements which could take into account, with the help of a unique basic equation called a Delta–Lognormal function, the major psychophysical phenomena reported in studies dealing with rapid movements. The theory has been found successful in describing the basic kinematic properties of velocity profiles as observed in finger, hand, arm, head, and eye movements. Professor Plamondon has studied and analyzed these biosignals extensively in order to develop creative and powerful methods and systems in various domains of engineering.

Full member of the Canadian Association of Physicists, the *Ordre des Ingénieurs du Québec*, the Union des Écrivaines et des Écrivains Québécois, Dr Plamondon is also an active member of several international societies. He is a Fellow of the Netherlands Institute for Advanced Study in the Humanities and Social Sciences (NIAS; 1989), of the International Association from Pattern Recognition (IAPR, 1994) and of the Institute of Electrical and Electronics Engineers (IEEE, 2000). From 1990 to 1997, he was the President of the Canadian Image Processing and Pattern Recognition Society and the Canadian representative on the board of Governors of IAPR. He has been the President of the International Graphonomics Society (IGS) from 1995 to 2007. He has been involved in the planning and organization of numerous international conferences and workshops and has worked with scientists from many countries. He is the Author or Co-author of more than 300 publications and owner of four patents. He has edited or co-edited four books and several special issues of scientific journals. He has also published a children book, a novel, and three collections of poems.